

THE PENNSYLVANIA STATE UNIVERSITY  
SCHREYER HONORS COLLEGE

DEPARTMENT OF ENGINEERING SCIENCE AND MECHANICS

DYE UPTAKE IN DYE SENSITIZED SOLAR CELLS

TANVI K THAKUR  
Fall 2011

A thesis  
submitted in partial fulfillment  
of the requirements  
for a baccalaureate degree  
in Engineering Science  
with honors in Engineering Science

Reviewed and approved\* by the following:

Mark W. Horn  
Professor in Engineering Science and Mechanics  
Thesis Supervisor

Christine M. Masters  
Associate Professor in Engineering Science and  
Mechanics  
Honors Adviser

Judith A. Todd  
Professor in Engineering Science and Mechanics  
P. B. Breneman Department Head

\* Signatures are on file in the Schreyer Honors College and Engineering Science and Mechanics office.

# Dye Uptake in Dye Sensitized Solar Cells

Tanvi Thakur

## **Abstract**

Dye-sensitized solar cells (DSSCs) represent a new frontier in solar cell technology. This study looks at the influence of N719 dye used within the cell. The dye forms a monolayer on the  $\text{TiO}_2$  surface and acts as source for the re-dex reaction that drives the cell. Using electrodes constructed from both structured thin film  $\text{TiO}_2$  and colloidal paste  $\text{TiO}_2$  upon conductive glass, cells were constructed and their efficiency was investigated.

# Contents

List of Figures	iii
List of Tables	v
Acknowledgements	vi
<b>1 Introduction</b>	<b>1</b>
<b>2 Literature Review</b>	<b>3</b>
2.1 Mechanism . . . . .	3
2.2 Layers of a DSSC . . . . .	4
2.2.1 Essential Components . . . . .	4
2.2.1.1 Conducting Glass Layer . . . . .	4
2.2.1.2 Nanocrystalline Film . . . . .	5
2.2.1.3 TiO <sub>2</sub> Nanolayer . . . . .	5
2.2.1.4 ZnO Nanolayer . . . . .	7
2.2.1.5 Dye Systems . . . . .	8
2.2.1.6 Electrolyte and Cathode . . . . .	9
<b>3 Methods</b>	<b>11</b>
3.1 Electrode Construction . . . . .	11
3.2 Adsorbed Dye Measurement . . . . .	13
3.3 Solar Cell Construction and Testing . . . . .	14
<b>4 Results and Discussion</b>	<b>15</b>
4.1 Dye Loading . . . . .	15
4.2 Photovoltaic Characterization . . . . .	16
4.3 Connection between dye loading photovoltaic characterization . . . . .	19
4.4 Sources of Error . . . . .	21
4.5 Future Work . . . . .	21
<b>Appendix</b>	<b>23</b>
<b>Bibliography</b>	<b>24</b>

## List of Figures

2.1	The light from the sun excites photons within the dye and causes a re-dox reaction within the cell[9]. . . . .	4
2.2	(a) and (c) show nanotubes before the application of titanium dioxide particles to increase the surface area. The results can be seen in (b) and (d)[13]. . . . .	6
2.3	The image on the left shows undecorated titanium dioxide nanotubes while the one on the right depicts the nanotubes after the titanium tetrachloride treatment. The post treatment nanotubes have a precipitate deposited on them [2] . . . . .	6
2.4	DSSC performance with and without a $\text{TiCl}_4$ treatment [1]. . . . .	7
2.5	The performance of a DSSC with two different types of dye (in black and red) along with a DSSC with no dye (blue)[5]. . . . .	8
2.6	Carbon nanotubes are effective as counter electrodes due to their long term stability[6]. . . . .	10
3.1	The deposition method for the STFs [12] . . . . .	12
3.2	A walk-through of the construction of the $\text{TiO}_2$ electrode: a) STF deposition b) definition of the nominal area c) dye loading on the defined area . . . . .	12
3.3	A walk-through of the construction of the cell: a) $\text{TiO}_2$ STF with defined area and dye adsorbed b) Parafilm spacer with window cut out c) Platinum counter electrode. Electrolyte must be added to the active area to complete the circuit. . . . .	14
4.1	A chart showing the absorption peaks along a portion of the visible spectrum. Between 300 and 350 nm, the cuvette displays a high amount of absorption; this particular peak is disregarded because it does not show absorption by the dye. Sample properties listed in table (1). . . . .	16
4.2	A comparison of STF (left) and colloidal (right) geometries [12]. . . . .	17
4.3	A look at how the geometry of the $\text{TiO}_2$ anode can affect the efficiency of the cell. Sample properties listed in table (1). . . . .	17
4.4	IV Curves for slurry cells tested with differing platinum electrodes. Sample properties listed in table (1). . . . .	18
4.5	IV Curves for STF cells tested with differing platinum electrodes. Sample properties listed in table (1). . . . .	19

4.6	A connection is drawn between the dye molecules per unit volume and the fill factor of the cell. Samples in blue have a single coat, the one in purple has a double coat, those in green have a triple coat and the ones in yellow are slurry cells. No samples have an underlayer. The vertical axes represent the number of molecules per m <sup>3</sup> (left) and fill factor (right) for the cells tested with the given sample. Sample properties listed in table (1).	20
4.7	All samples have a double coat. Those in green have an underlayer while those in purple and blue do not. The vertical axes represent the number of molecules per m <sup>3</sup> (left) and fill factor (right) for the cells tested with the given sample. Sample properties listed in table (1).	20
4.8	The purple samples have an underlayer while those in green do not. The vertical axes represent the number of molecules per m <sup>3</sup> (left) and fill factor (right) for the cells tested with the given sample. Sample properties listed in table (1).	21

## List of Tables

2.1	The effects of pore size on the efficiency of DSSC. Modified from [1]. . . .	9
1	Different samples and their physical properties . . . . .	23

## **Acknowledgements**

This thesis would not have been possible without the help of without the support of Dr. Mark W. Horn in addition to the help of Sean M. Pursel and Hyeonseok Lee. Thank you for your guidance.

I would also like to thank the Department of Engineering Science and Mechanics at Penn State. Thank you for all your guidance and help over the years.

# Chapter 1

## Introduction

The massive flux of photons incident on the earth from the sun comprises an inexhaustible and plentiful energy source for the foreseeable future. In contrast to other renewable resources whose globally extractable power is less than 5 TW, the solar constant on the Earth's surface is 120 000 TW[8].

The traditional solar cells that we are familiar with are akin to dinosaurs - big and clunky. While they have a very long life, the efficiency they work at is mediocre and the ability to integrate them into current housing design is limited at best. Traditional silicon photovoltaics use a p-n junction within the semiconductor material to capture energy from the sun. A new class of photovoltaics, dye-sensitized solar cells (DSSCs), is making use of inexpensive materials and fabrication processes to better harvest the bountiful solar energy. For homeowners that do want to be more environmentally friendly but do not want to end up with eye-sores on their roofs or in their backyards, dye-sensitized solar cells are the way of the future. Their transparent appearance means that they can be integrated into the same space that has eluded traditional photovoltaics for so long - windows. The low manufacturing costs mean that integrating them into buildings will no longer be an investment for the long-term. However, a drawback does exist - these new cells still do not have that efficiency of their dinosaur counterparts. But if there was even a modicum of increase in the efficiency, there would be no question about the winner of this solar battle.

It should come as no surprise then, that the winner of the 2010 Millennium Technology

Prize, the largest technology prize in the world, was Michael Grätzel, the inventor of the dye sensitized solar cell. His company, G24 Innovations, and others, such as Dyesol, are working towards making this technology available worldwide.

One major benefit to dye sensitized solar cells is that they can be manufactured on flexible substrates. This can lead to solar-powered devices where solar cells have never been before - on our laptops, clothes and possibly even cars. As with every technology before it, there are problems that need to be addressed. However, with further research the possibilities are endless.

## Chapter 2

### Literature Review

#### 2.1 Mechanism

Michael Grätzel, the inventor of the DSSC, cites photosynthesis as his inspiration for this technology[4]. In theory, DSSCs work in a very similar way to leaves of a plant when they convert the sun's energy to electricity. Sandwiched between two very thin, transparent electrodes are a layer of dye and an electrolyte. One of the most novel features of the DSSC is that it is transparent. It uses this transparency to its advantage by absorbing light that falls upon both sides of the cell.

Once the dye is hit by sunlight, the electrons within are excited through the adsorption of photons. The excited electrons are injected into the nanocrystalline film that is part of the anode and the dye is oxidized. The electrolyte, the final part of this photovoltaic sandwich, then comes into play. It reduces the oxidized dye and returns it to the original state[7]. This reaction, which happens millions of times over and allows for charge to flow, can be seen in figure (2.1). The nanocrystalline thin film, a  $\text{TiO}_2$  colloid in this case, is coated with small red particles of dye which absorb the light from the sun.

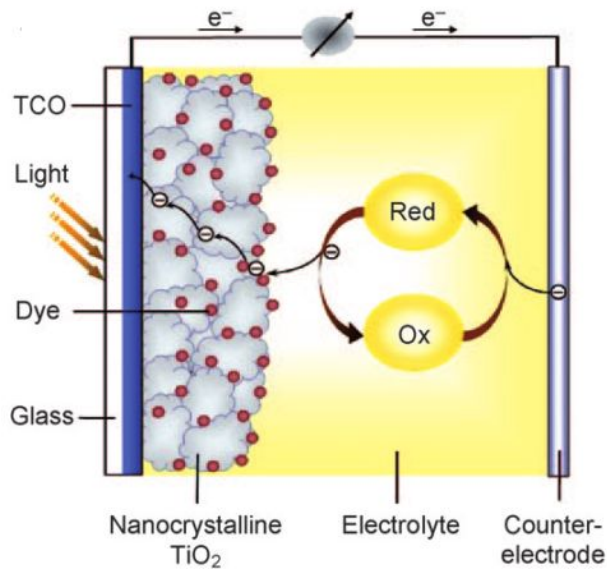


Figure 2.1: The light from the sun excites photons within the dye and causes a re-dox reaction within the cell[9].

## 2.2 Layers of a DSSC

### 2.2.1 Essential Components

A simple dye-sensitized solar cell consists of the following components in the given order:

- Conducting glass layer
- Nanocrystalline film
- Monolayer of dye
- Electrolyte
- Cathode

Utilizing this very basic structure, we can create solar cells that harvest energy from the sun[4]. In addition, increasing the efficiency of the solar cell is dependent on changes that are made to these specific components.

#### 2.2.1.1 Conducting Glass Layer

The glass layer is useful in two main ways - it provides a transparent substrate for the DSSCs and it completes the electric circuit that is formed by the layers of the DSSCs.

Most DSSCs use fluorine-doped tin-oxide thin film as the transparent conducting oxide (TCO) for the conducting glass[2]. The use of indium tin-oxide has also been explored[15]. One drawback is that the resistance of these metal-oxide-based thin films increases by one order of magnitude with the annealing step necessary to crystallize the nanotube array. These metal oxide based conductors can be unstable in the presence of an acid or base like the electrolytes used within these cells so further research is being done for more flexible as well as more stable transparent electrodes. A new possibility is the use of thin, transparent and electrically-conductive graphene. While both thermally and electrically stable, the performance of the graphene is slightly lower than that of the metal oxide coated glass[15]. With further research, it is possible that graphene's excellent electrical properties will help it excel in this competition.

#### **2.2.1.2 Nanocrystalline Film**

One of the most important aspects of the DSSC, the nanocrystalline film provides the site for the oxidation-reduction reaction to take place. It must be a structured film of some sort, either in the form of nanoparticles, nanotubes, nanowires, nanorods, sculptured-thin films or even nanofibers. This is done to ensure that the surface area available for chemisorption between the film and the monolayer of dye is at a maximum. The actual surface area for such a structured film can be over 1000 times the apparent surface area[14]. In addition, enhancements can be made to the structured thin film to increase its surface area further. Figure (2.2) shows the use of  $\text{TiO}_2$  nanoparticles to 'decorate' the  $\text{TiO}_2$  nanotubes[13]. In addition, these films are sintered so that necking occurs between the particles allowing for channels that enable electron transport[14]. The most commonly used materials for this layer are either  $\text{TiO}_2$  or  $\text{ZnO}$ . There are distinct advantages and disadvantages to each as detailed in the sections below.

#### **2.2.1.3 $\text{TiO}_2$ Nanolayer**

$\text{TiO}_2$  is widely used for this type of cell because it is cheap, widely available and non-toxic. It exists in three mineral forms or crystal structures: anatase, rutile, and brookite.

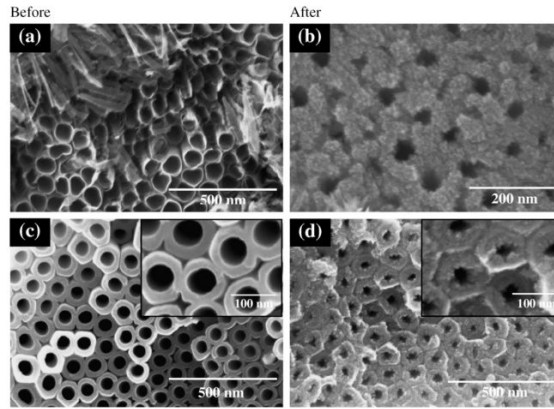


Figure 2.2: (a) and (c) show nanotubes before the application of titanium dioxide particles to increase the surface area. The results can be seen in (b) and (d)[13].

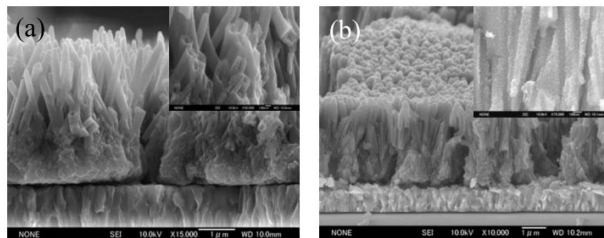


Figure 2.3: The image on the left shows undecorated titanium dioxide nanotubes while the one on the right depicts the nanotubes after the titanium tetrachloride treatment. The post treatment nanotubes have a precipitate deposited on them [2]

Of the three, the anatase phase of the  $\text{TiO}_2$  is most commonly used. However, recent research has investigated the rutile phase given its superior light-scattering properties and inexpensive cost[10].

As discussed earlier, the films are sintered to create 'necks' between the particles. This effect can be further increased with the addition of titanium tetrachloride ( $\text{TiCl}_4$ )[1]. While the treatment does decrease the surface area of the film, the  $\text{TiCl}_4$  deposits itself at the interparticle neck and thus increases the overall current that can be collected in the DSSC[1]. Figure (2.3) depicting the addition of the  $\text{TiCl}_4$  resembles figure (2.2)b & d (in terms of a precipitate on the nanotubes) but the key mechanism here is different. Figure (2.4) shows the improvement in the performance that the solar cell experiences after the  $\text{TiCl}_4$  treatment. On the x-axis, the wavelength along which absorption of light occurs

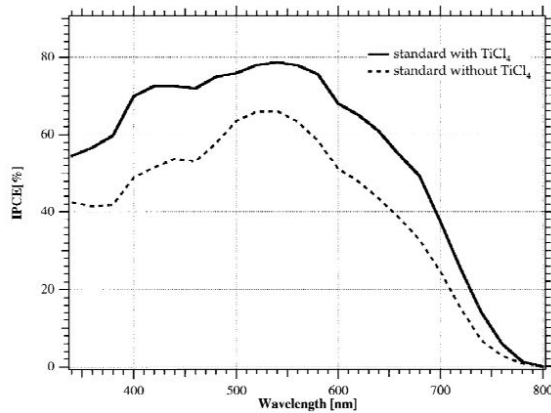


Figure 2.4: DSSC performance with and without a  $\text{TiCl}_4$  treatment [1].

is shown; on the y-axis, the incident photon conversion efficiency (IPCE), the percentage of incident photons that get converted to electrons, is shown. IPCE is important because it measures how effective a solar cell is in the given light- the higher a DSSC's ICPE, the higher its overall efficiency[1]. The biggest issue that arises with the  $\text{TiO}_2$  is the extremely slow electron escape time (1-10ms for  $10\mu\text{m}$  thick films). A slower electron escape time can affect efficiency significantly[3].

#### 2.2.1.4 ZnO Nanolayer

Both ZnO and  $\text{TiO}_2$  films rely on trap-limited diffusion for their transport. While the  $\text{TiO}_2$  is much better at handling a degraded dye solution, its slower electron escape times mean that the cell does not reach its potential maximum efficiency[3]. ZnO, a wide band gap semiconductor, allows for a faster transport through the use of 1-D nanowires. These nanowires allow for the electron to pass through the path formed via the nanowire rather than jumping between nanoparticles. The main reason that this method is better suited for ZnO rather than  $\text{TiO}_2$  is that  $\text{TiO}_2$  nanowires are very difficult to synthesize uniformly[3]. Problems arise with the ZnO electrodes because they increase the speed at which the dye used within the DSSC degrades. As discussed in the next section, dye degradation is one of the limitations that must be overcome for the widespread use of

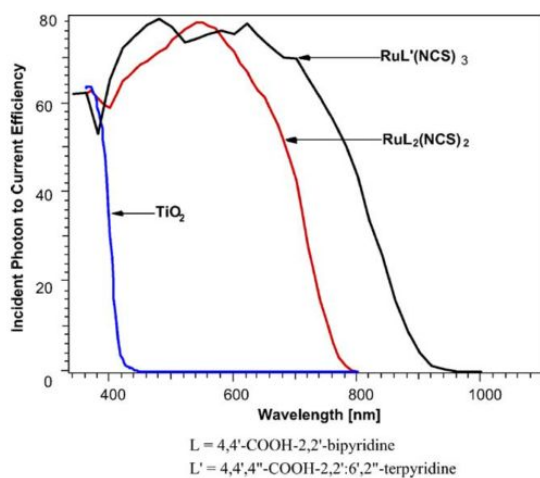


Figure 2.5: The performance of a DSSC with two different types of dye (in black and red) along with a DSSC with no dye (blue)[5].

DSSCs.

### 2.2.1.5 Dye Systems

The most commonly used dye within the solar cells is a ruthenium-based dye in the form of either N719 or N3. These dyes have shown the highest efficiencies thus far at around 11%[11]. The success of a dye depends on how much of the electromagnetic spectrum it is capable of absorbing. As shown in figure (2.5), titanium films (marked in blue) alone only absorb in the ultraviolet region, meaning that with no dye these cells would be woefully inefficient[5].

The two dyes depicted in figure (2.5) are N3 (dye L in red) and black dye (dye L' in black), both ruthenium-based dyes. Again, the y-axis for this graph uses IPCE as a measure of efficiency. Ruthenium-based dyes increase this efficiency by absorbing within the 400-500nm range, right at the beginning of the visible spectrum.

One of the biggest problems is that the ruthenium-based dyes are only stable when they are not in the oxidized state. Upon oxidation, which happens millions of times throughout the life of the DSSC, the dye loses sulfur and starts to degrade rapidly[5]. This

decreases the life of the DSSC significantly. In contrast, the traditional silicon solar cells have an average life-span of 20 years which is over twice that of DSSCs[4].

An ideal dye would absorb at all wavelengths of visible, infrared and ultraviolet light. If a dye were to absorb some parts of the ultra-violet or the infrared spectrum as well, it would increase overall DSSC efficiency. Till now, such a dye has been difficult to find. Instead scientists are looking towards using a system of multiple dyes to achieve higher efficiencies. In addition, the use of organic dyes is also becoming increasingly popular. Organic dyes refer to dyes found in nature; studies have been done using different types of teas, berry juices and even plant materials. Organic dyes are cheaper in the long run and more easily available than ruthenium-based dyes[11].

### 2.2.1.6 Electrolyte and Cathode

The electrolyte used is one of the critical components in mass manufacture of DSSCs. As most electrolytes are liquid in form, sealing the solar cell is a critical issue. In this and related work, organic liquid electrolytes were used[12]. These resulted in a higher efficiency but the long-term stability was compromised[16]. When solid-state and quasi-solid-state electrolytes were used in previous work, they were inefficient due to their inability to penetrate the nanocrystalline network[12]. Pore size, the diameter of the nano-sized holes within the porous thin film, also played a key-role in helping increase efficiency. Below a certain threshold, the increase in surface area from a smaller pore is ineffective at mitigating the pore's negative effects on the electrolyte[1]. Table (2.1) shows that at a smaller pore size, the efficiency of the DSSC is lower. In addition, an increase in the amount of sunlight that hits the cell does not help alleviate these effects.

Table 2.1: The effects of pore size on the efficiency of DSSC. Modified from [1].

Sun Estimate	$I_{SC}$	$V_{OC}$	Efficiency (%)
Electrode with average pore size of 4nm			
$\frac{1}{10}$ Sun	1.4	550	4.72
1 Sun	9.2	620	3.38
Electrode with average pore size of 20nm			
$\frac{1}{10}$ Sun	1.3	560	4.9
1 Sun	12.1	630	5

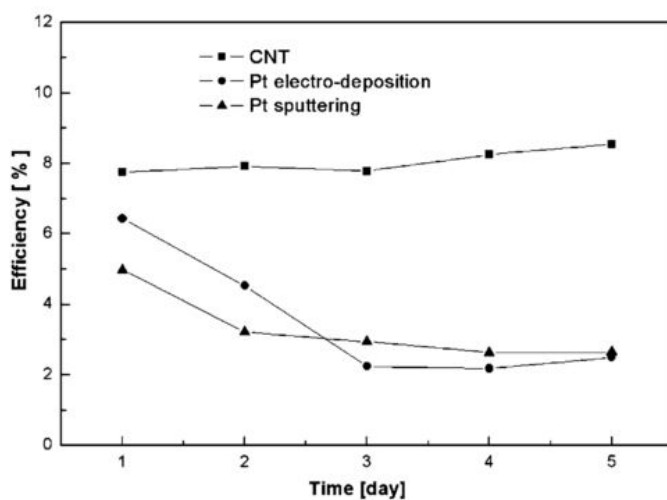


Figure 2.6: Carbon nanotubes are effective as counter electrodes due to their long term stability[6].

The counter electrodes used within a DSSC need to have a high electrical conductivity. Thus far, the most commonly used counter electrodes have been platinum films on TCO glass. But for mass manufacture, platinum electrodes can drive up the costs of DSSCs so a cheaper alternative is ideal. Carbon nanotubes (CNT) are both inexpensive and excellent conductors making them ideal candidates for use in counter electrodes. Figure (2.6) shows that CNT actually help reduce the degradation of the DSSC that can be caused from the reaction between the electrolyte and the platinum electrode.

## Chapter 3

### Methods

In order to characterize the dye uptake, measurements were made to record the nature of the STFs. These measurements include thickness, dye loading and cell performance.

#### 3.1 Electrode Construction

FTO-glass substrates were immersed in isopropanol and then immersed in ethanol. The substrate was then rinsed with deionized water and allowed to air dry. A TiO<sub>2</sub> structured thin film was deposited onto the FTO using a dual electron beam evaporator. The thin film is columnar in nature with an angle of 10° between the substrate plane and the vapor flux direction. This angle,  $\chi_v$ , was created using a wedge holder. The thickness of the TiO<sub>2</sub> films was measured using a Tencor P-10 profilometer. The measurement was further refined using a LEO-1530 field emission scanning electron beam microscope. Since the crucible holds a limited amount of material, the samples were often coated twice or three times in order to increase the thickness of the photoanode

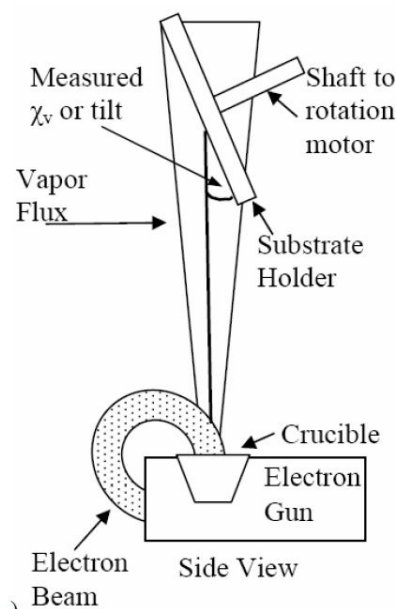


Figure 3.1: The deposition method for the STFs [12]

In order to provide a comparison, colloidal paste electrodes were also made using a commercial paste. The paste was spread onto the FTO-glass using a glass slide. The paste was soft baked at 80° C for 20 minutes. All samples were annealed at 450° C for 6 hours in O<sub>2</sub> before going into the dye solution as described below. Upon removal, the sample was rinsed with acetonitrile to remove excess dye. The platinum counter electrode was made using FTO-glass coated with a Cr/Pt layer. A drop of 0.5mM chloro-hexaplatinic acid was added to the surface of the counter electrode. It should be noted that the counter electrodes experienced degradation if they were not used promptly.

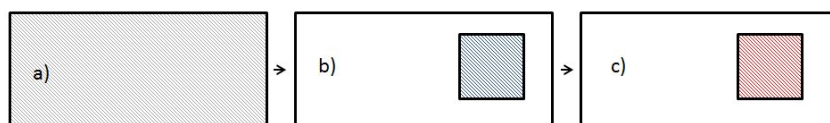


Figure 3.2: A walk-through of the construction of the TiO<sub>2</sub> electrode: a) STF deposition b) definition of the nominal area c) dye loading on the defined area

## 3.2 Adsorbed Dye Measurement

Dye loading was measured by sensitizing known nominal areas of the TiO<sub>2</sub> STF with N719 dye. The amount of TiO<sub>2</sub> within each sample was regulated by limiting the total area over which the film was present as seen in figure (3.2). This was done by using a doctor blade to scrape the TiO<sub>2</sub> STF outside of a 5mm × 5mm area off the FTO substrate. The sample was immersed in the dye solution (0.3mM solution of N719 in a mixture of acetonitrile and tert-butanol). Desorption of the dye occurred after testing when the sample was immersed in 5ml of 0.1M NaOH solution. A 1ml sample of the desorption solution was transferred to a cuvette. Scattering from excess TiO<sub>2</sub> particles was reduced with the addition of 1-2 drops of 9% wt HF added to each cuvette. Though the HF resulted in the formation of a precipitate in cold weather, it is not thought to affect the dye measurements. Dye concentration was measured in solution with a Perkins Elmer 950 spectrometer using a cuvette holder and the standard detector. Measurements were typically made on a range of 300 to 800nm. The Beer-Lambert formula (3.1) was used to determine the atoms of dye present on the surface of the TiO<sub>2</sub> STF. The formula states:

$$A = \epsilon \times b \times c \quad (3.1)$$

where

$A$  =absorbance

$\epsilon$  = wavelength dependent absorptivity coefficient

$b$  = path length

$c$  = analyte concentration

Absorbance  $A$  was measured by the UV-VIS spectrophotometer. Values of  $\epsilon$  were found within literature[9]. The path length  $b$  was the length of the cuvettes used. Analyte concentration  $c$  was solved for and was used to determine the atoms of dye present on the given sample.

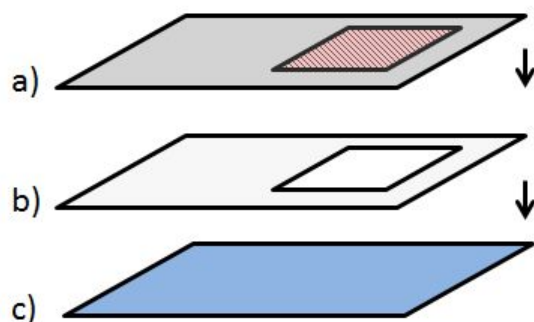


Figure 3.3: A walk-through of the construction of the cell: a) TiO<sub>2</sub> STF with defined area and dye adsorbed b) Parafilm spacer with window cut out c) Platinum counter electrode. Electrolyte must be added to the active area to complete the circuit.

### 3.3 Solar Cell Construction and Testing

A spacer made from stretched Parafilm ( $40\mu\text{m}$ ) was applied to the TiO<sub>2</sub> layer to maintain an equal distance between the two electrodes. A window cut into the Parafilm allowed for the completion of the circuit. Four drops of the electrolyte were added to the active area of the electrode surface and allowed to dry. Drops were added till the thickness of the electrolyte was equal to that of the spacer. A counter electrode of evaporated platinum on FTO was then clamped into place and the cell was tested. Contact was made using alligator clips. Given the temporary nature of the sealing process, cells had to be tested immediately after they were created. Current-voltage measurements (IV) were done on an automated system from Newport at 1 Sun. Intensity was calibrated using a reference silicon cell from Newport. The software provided collected 60 data points in 6 seconds and calculated necessary parameters automatically.

## Chapter 4

### Results and Discussion

This section details the results of the dye loading and photovoltaic characterization of the TiO<sub>2</sub> STF's used within the DSSC. The properties of the samples used within the current section are listed within table (1) in the appendix.

#### 4.1 Dye Loading

Dye loading is useful in identifying how effective a DSSC can be. Because it looks at absorption by the dye across the entire visible spectrum, it can show which dye is most effective for certain lights. In figure (4.1), we see peaks in the violet end of the spectrum as well as towards the middle. Ideally a dye would absorb throughout the spectrum for the most effective DSSC. It is important to note that absorbance by the desorbed dye alone cannot predict the performance of the cell. Given that different STF's have a different thickness, one must observe the dye molecules present per unit volume of STF. Normalized dye uptake can be directly linked to the short circuit current ( $I_{SC}$ ) obtainable in a cell because each dye molecule is theoretically capable of photovoltaic conversion.

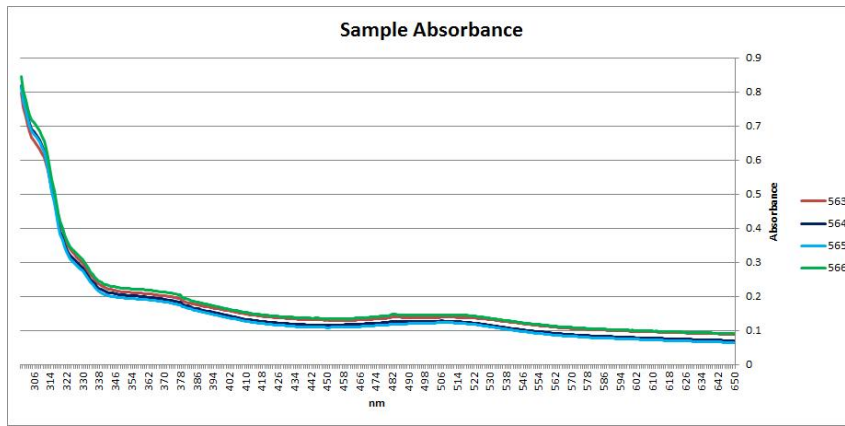


Figure 4.1: A chart showing the absorption peaks along a portion of the visible spectrum. Between 300 and 350 nm, the cuvette displays a high amount of absorption; this particular peak is disregarded because it does not show absorption by the dye. Sample properties listed in table (1).

## 4.2 Photovoltaic Characterization

Fill factor for a solar cell is the ratio of its theoretical maximum power output and the product of its open circuit voltage ( $V_{OC}$ ) and its short circuit current ( $I_{SC}$ ). Two solar cells having the same  $V_{OC}$  and  $I_{SC}$  could have drastically different fill factors. This can be seen in figure (4.4) where samples A1 and A4 are close in terms of  $V_{OC}$  and  $I_{SC}$  but have fill factors of 50.26% and 47.34% respectively because their theoretical maximum power values are different. A simple way to visualize fill factor is to look at the rectangle constructed from the x-intercept and the y-intercept from the peak of the curve and compare it to the rectangle created from the actual x-intercept and y-intercept of the curve.

Looking at figure (4.2), it is evident that there exists a difference in the surface geometries of colloidal cells and STF cells. One important factor to investigate is if one allows for a better performance than the other. With figure (4.3), the effect of the use of STF on cells seems to be positive. However, given the presence of the underlayer, it is difficult to say in this study whether the performance is based solely on the geometries of the  $TiO_2$ .

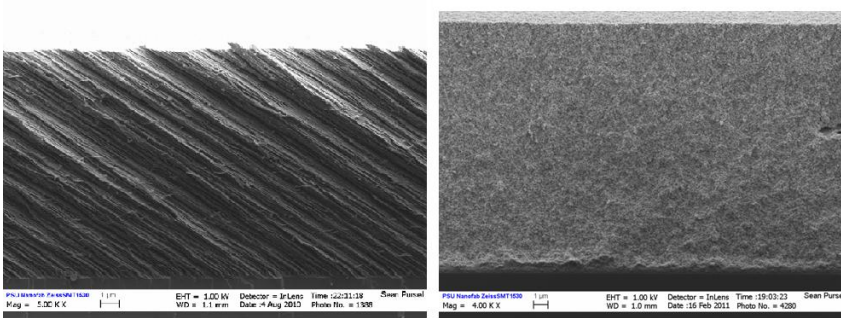


Figure 4.2: A comparison of STF (left) and colloidal (right) geometries [12].

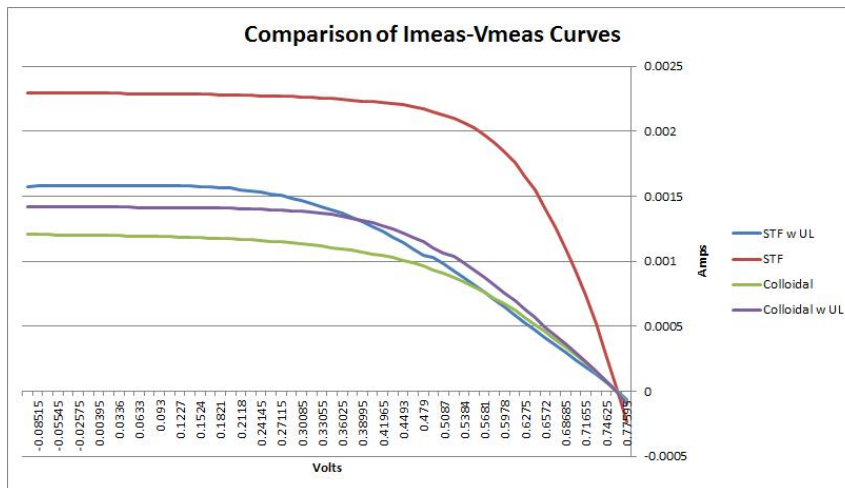


Figure 4.3: A look at how the geometry of the  $\text{TiO}_2$  anode can affect the efficiency of the cell. Sample properties listed in table (1).

Another aspect of DSSCs that was evaluated in this thesis work was the effect of platinum cathode degradation. As seen in figure (4.4), the effects of an older platinum electrode are very detrimental. All the slurry cells were prepared from the same commercial paste using the same method. However, a larger gap of time passed between the preparation of the platinum electrode and the testing of the prepared cell for the sample C1 than for the samples A1 and A4. As a result, the samples A1 and A4 have a much higher fill factor and thus a higher efficiency.

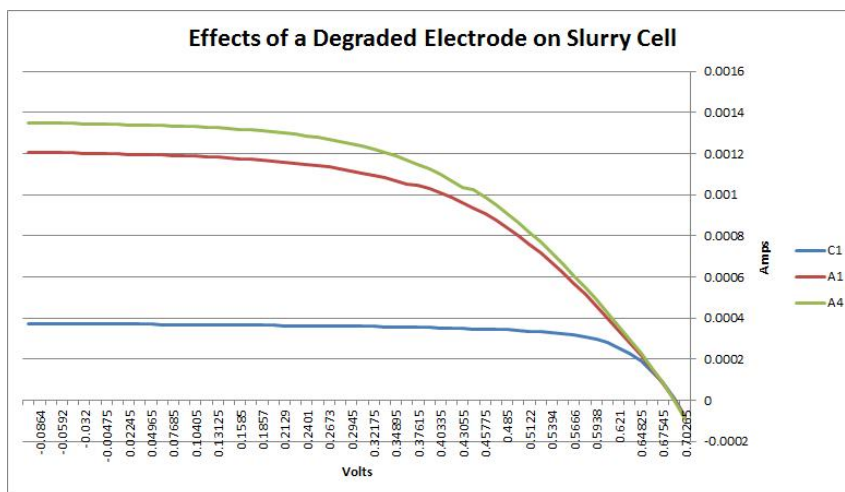


Figure 4.4: IV Curves for slurry cells tested with differing platinum electrodes. Sample properties listed in table (1).

Similarly, in figure (4.5) the effect is also visible. All four cells have no underlayer. CN1 and CN3 were tested with an electrode that had been prepared much earlier and show degradation in performance in comparison to cells prepared from 552 and 553.

This result points to a flaw in this particular method of cell construction. While it is fast and easy to construct, the resultant cell has a very small window for optimal performance. With these tests, it is fairly evident that this would not be a commercially viable method for cell construction.

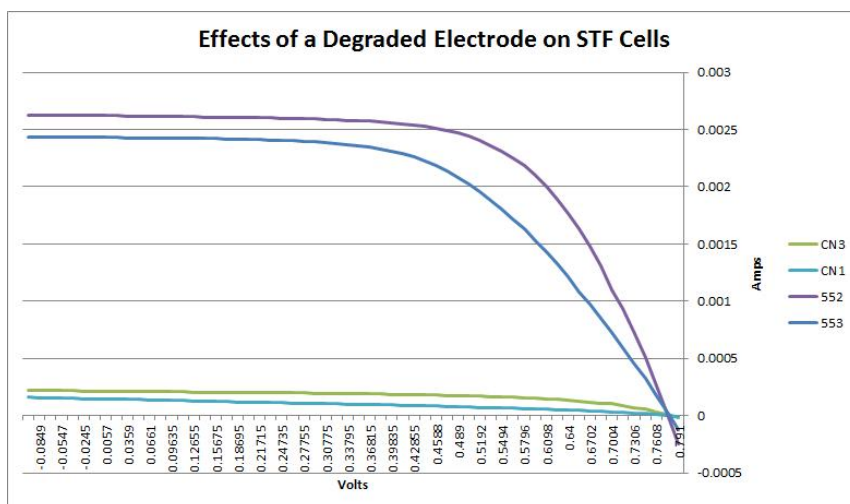


Figure 4.5: IV Curves for STF cells tested with differing platinum electrodes. Sample properties listed in table (1).

### 4.3 Connection between dye loading photovoltaic characterization

In figure (4.6) above there is no clear correlation between the thickness of the film which affects the number of dye molecules per  $m^3$  and the fill factor. While a trend can be seen in samples with one coat and three coats (blue and green respectively), the sample with two coats (purple) does not support this trend. In comparison, the slurry cells have the lowest dye molecule concentration but not necessarily the lowest fill factor. In figure (4.7) the samples for the double coats which do not have an underlayer are limited (blue). They do indicate, within this very small sample size, that the presence of an underlayer may lead to a lower fill factor. The results indicate that differences in concentration of dye molecules do not necessarily coincide with how high or low the fill factor is. Unlike samples before them, those in figure (4.8) indicate a very clear trend. The presence of an underlayer (purple samples) has led to a decrease in the fill factor. Alternately, even a significant decrease in the dye molecule concentration has not decreased the efficiency of the cells. The data indicates that sample 560 actually reflects light at this given wavelength but still outperforms three of the four cells with underlayers. One explanation for this may be

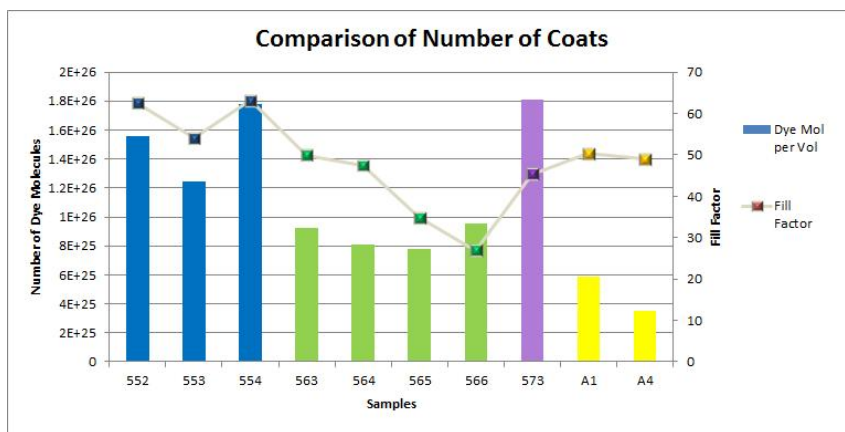


Figure 4.6: A connection is drawn between the dye molecules per unit volume and the fill factor of the cell. Samples in blue have a single coat, the one in purple has a double coat, those in green have a triple coat and the ones in yellow are slurry cells. No samples have an underlayer. The vertical axes represent the number of molecules per  $\text{m}^3$  (left) and fill factor (right) for the cells tested with the given sample. Sample properties listed in table (1).

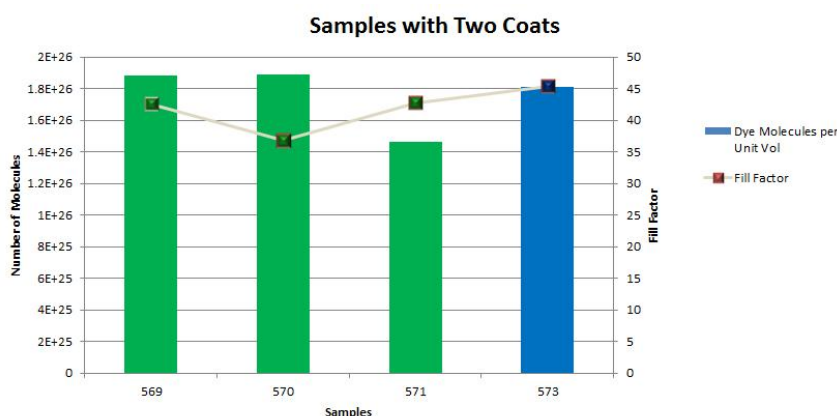


Figure 4.7: All samples have a double coat. Those in green have an underlayer while those in purple and blue do not. The vertical axes represent the number of molecules per  $\text{m}^3$  (left) and fill factor (right) for the cells tested with the given sample. Sample properties listed in table (1).

that the dye molecule concentration was calculated only at a wavelength of 530nm- the wavelength at which the extinction coefficient used was recorded. It is entirely possible that the four samples without underlayers (in green) performed poorly at this wavelength but absorbed light well at other points within the spectrum.

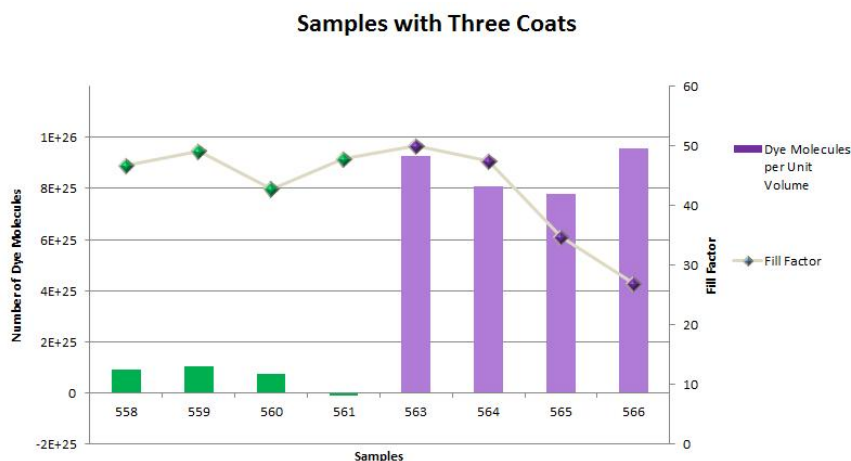


Figure 4.8: The purple samples have an underlayer while those in green do not. The vertical axes represent the number of molecules per  $\text{m}^3$  (left) and fill factor (right) for the cells tested with the given sample. Sample properties listed in table (1).

#### 4.4 Sources of Error

One of the main sources of error within the experiment is the thickness measurement of the film. Thickness was measured for one sample within the batch. This may have led to an inaccurate volume for the films and thus, an inaccurate value for the dye molecules per unit volume within the film. Another source of error is the process through which the active area within the film is defined. Because it was done using a doctor blade, it is possible that the  $5\text{mm} \times 5\text{mm}$  area defined may be inaccurate. It is also possible that there was additional STF on the edges of the FTO that absorbed dye in addition to the defined area of the STF. This could lead to a higher value for the number of dye molecules for a given sample.

#### 4.5 Future Work

More investigation needs to be done in order to definitively link the dye uptake of DSSCs with their performance. One method of accomplishing this would be to compare surface area measurements for different types of STFs and calculating the dye molecules per unit area and unit volume. Another variable to look into would be the platinum counter electrode. It is important to see the role played by the prepared electrode in the

performance of the cell. It may be possible to set up an experiment that tests different counter electrodes with a DSSC counterpart. This would help improve understanding about long-term stability of DSSCs.

## Appendix

Table 1: Different samples and their physical properties

Sample Name	Type	Number of Coatings	Underlayer Present
552	STF	1	No
553	STF	1	No
554	STF	1	No
555	STF	1	No
556	STF	1	No
557	STF	1	No
558	STF	3	Yes
559	STF	3	Yes
560	STF	3	Yes
561	STF	3	Yes
563	STF	3	No
564	STF	3	No
565	STF	3	No
566	STF	3	No
569	STF	2	Yes
570	STF	2	Yes
571	STF	2	Yes
573	STF	2	No
A1	Colloidal	-	No
A4	Colloidal	-	No
AUL1	Colloidal	-	Yes
AUL4	Colloidal	-	Yes
C1	Colloidal	-	No
C3	Colloidal	-	No
CN1	STF	1	No
CN3	STF	1	No

## Bibliography

- [1] Christophe J Barbe, Francine Arendse, Pascal Comte, Marie Jirousek, Frank Lenzmann, Valery Shklover, and Michael Gra. Nanocrystalline Titanium Oxide Electrodes for Photovoltaic Applications. *Synthesis*, 71:3157–3171, 1997.
- [2] Patcharee Charoensirithavorn, Yuhei Ogomi, Takashi Sagawa, Shuzi Hayase, and Susumu Yoshikawa. Improvement of Dye-Sensitized Solar Cell Through  $\text{TiCl}_4$ -Treated  $\text{TiO}_2$  Nanotube Arrays. *Journal of The Electrochemical Society*, 157(3):B354, 2010.
- [3] An-Jen Cheng, Yonhua Tzeng, Yi Zhou, Minseo Park, Tsung-hsueh Wu, Curtis Shannon, Dake Wang, and Wonwoo Lee. Thermal chemical vapor deposition growth of zinc oxide nanostructures for dye-sensitized solar cell fabrication. *Applied Physics Letters*, 92(9):092113, 2008.
- [4] M Gratzel. Dye-sensitized solar cells. *Journal of Photochemistry and Photobiology C: Photochemistry Reviews*, 4(2):145–153, October 2003.
- [5] M Gratzel. Conversion of sunlight to electric power by nanocrystalline dye-sensitized solar cells\*1. *Journal of Photochemistry and Photobiology A: Chemistry*, 164(1-3):3–14, June 2004.
- [6] Bo-Kun Koo, Dong-Yoon Lee, Hyun-Ju Kim, Won-Jae Lee, Jae-Sung Song, and Hee-Jae Kim. Seasoning effect of dye-sensitized solar cells with different counter electrodes. *Journal of Electroceramics*, 17(1):79–82, September 2006.

- [7] Hong Lin, Wen-li Wang, Yi-zhu Liu, Xin Li, and Jian-bao Li. New trends for solar cell development and recent progress of dye sensitized solar cells. *Frontiers of Materials Science in China*, 3(4):345–352, September 2009.
- [8] Alex B F Martinson, Thomas W Hamann, Michael J Pellin, and Joseph T Hupp. New architectures for dye-sensitized solar cells. *Chemistry (Weinheim an der Bergstrasse, Germany)*, 14(15):4458–67, January 2008.
- [9] Amaresh Mishra, Markus K R Fischer, and Peter Bäuerle. Metal-free organic dyes for dye-sensitized solar cells: from structure: property relationships to design rules. *Angewandte Chemie (International ed. in English)*, 48(14):2474–99, January 2009.
- [10] K Park and M Dhayal. High efficiency solar cell based on dye sensitized plasma treated nano-structured TiO<sub>2</sub> films. *Electrochemistry Communications*, 11(1):75–79, January 2009.
- [11] Mariachiara Pastore, Edoardo Mosconi, Filippo De Angelis, and Michael Graätzel. A Computational Investigation of Organic Dyes for Dye-Sensitized Solar Cells: Benchmark, Strategies, and Open Issues. *The Journal of Physical Chemistry C*, 114(15):7205–7212, April 2010.
- [12] Sean M Pursel. *Dye Sensitized Solar Cells Based On Nanowire Sculptured Thin Film Titanium Dioxide Photoanodes*. PhD thesis, The Pennsylvania State University, 2011.
- [13] Poulomi Roy, Doohun Kim, Indhumati Paramasivam, and Patrik Schmuki. Improved efficiency of TiO<sub>2</sub> nanotubes in dye sensitized solar cells by decoration with TiO<sub>2</sub> nanoparticles. *Electrochemistry Communications*, 11(5):1001–1004, May 2009.
- [14] G Tulloch. Light and energy dye solar cells for the 21st century. *Journal of Photochemistry and Photobiology A: Chemistry*, 164:209–219, May 2004.
- [15] Xuan Wang, Linjie Zhi, and Klaus Müllen. Transparent, conductive graphene electrodes for dye-sensitized solar cells. *Nano letters*, 8(1):323–7, January 2008.

- [16] Yong Zhao, Xianliang Sheng, Jin Zhai, Lei Jiang, Chunhe Yang, Zhongwei Sun, Yongfang Li, and Daoben Zhu. TiO(2) porous electrodes with hierarchical branched inner channels for charge transport in viscous electrolytes. *Chemphyschem : a European journal of chemical physics and physical chemistry*, 8(6):856–61, April 2007.

# Academic Vita Of Tanvi K. Thakur

tanvi@psu.edu  
610 945 6995  
24 Cabot Court  
Wayne, PA 19087

---

## *Education:*

The Pennsylvania State University

University Park, PA

- Bachelor of Science in Engineering Science, Fall 2011
- *Honors:* Schreyer Honors College Scholar, Honors Curriculum in Engineering, Dean's List
- *Involvement:* Society for Engineering Science, Women in Engineering, Penn State THON

Peking University

Beijing, China

Summer 2009

- Analyzed differential equations using L-U decomposition methods
- Presented projects with a team of Chinese students

## *Experience:*

Honors Thesis: Dye Uptake in Dye-Sensitized Solar Cells

University Park, PA

Fall 2010 – Present

- Collected and analyzed dye adsorption data for sculptured thin films
- Tested efficiency of solar cell prototypes

Liberty Mutual

Dover, NH

Summer 2010

Summer Intern

- Assisted Enterprise Architecture and Application Services department with annual budget process
- Organized and prepared 2011 budget exhibits
- Created 100 page budget book that was presented to different internal IT departments

Penn State Learning

University Park, PA

October 2009 – Present

Tutor

- Review material from Math 002 – 251 with a focus differential equations and linear algebra
- Lead guided study groups and review sessions of up to 30 students on a regular basis